

Influence of Process Parameters on Porosity Behaviour of Laser Metal Deposited Titanium Composites

Musibau O. Ogunlana, and Esther T. Akinlabi, *Member, IAENG*

Abstract—This research paper reports the effect of laser power on the degree of porosity of the deposited tracks and characterized the specific porous structures of the deposits. The samples were characterized through the microstructure and the porosity analysis. The results revealed that as the laser power was increased, the degree of porosity was however reduced. Prior the characterization process, titanium alloy and boron carbide (Ti6Al4V-B₄C) composites powder were deposited on Ti6Al4V substrate using laser metal deposition (LMD) process through the application of Ytterbium fibre laser system. The laser power was varied between 800 W and 2400 W at interval of 200 W while all other process parameters were kept constant. The maximum capacity of this laser system is 3.0 KW which provides beam size of 4 mm for the control characterization of the deposited samples. The porosity behaviour of various samples at different laser power were observed in which the degree of their porosities varies as the laser power increases. At a laser power of 2200 W, there was no porosity observed in the composite which revealed that there were no unmelted powder presented in the melt pool after solidification for this particular sample. Percentage porosity was significantly reduced from 0.45% to 0.03%.

Index Terms—Boron carbide, Laser power, Porosity, Processing parameters, Titanium alloy

I. INTRODUCTION

THIS paper presents the report on the influence of process parameters on the characterization of porosity behaviour of titanium composites and its relationship with the increasing laser power of laser metal deposition (LMD) process. LMD is an additive manufacturing technology of solid freeform fabrication used in the manufacture of solid components. This includes the variety of applications such as surface coating, repair of worn-out or damaged high-value components, and rapid manufacture of medical components. Whereas, additive manufacturing is the process of joining materials to create objects from digital three-dimensional (3-D) model [1]-[3].

Manuscript received July 01, 2016; revised August 08, 2016.

Musibau O. Ogunlana is a Masters Candidate in the Department of Mechanical Engineering Science, University of Johannesburg, Auckland Park Kingsway Campus, Johannesburg, South Africa, 2006. (E-mail: 201510083@student.uj.ac.za or emmbbyola@gmail.com).

Prof Esther T. Akinlabi is a Professor and the Head of Department in the Department of Mechanical Engineering Science, University of Johannesburg, Auckland Park Kingsway Campus, Johannesburg, South Africa, 2006. Phone: +2711-559-2137, (E-mail: etakinlabi@uj.ac.za).

During the LMD process, powder is fed into the melt pool created by laser beam onto the surface of the substrate. The heat generated by the melt pool together with the laser beam causes the powder to melt and bond with the substrate. Subsequently, the solidification of the melt pool and a deposited solid track material is left on the laser path. However, this process is repeated layer after layer until the buildup process is completed [3], [4].

LMD process has various applications, such as: the production of prototypes, functionally graded materials, and medical implants. Consequently, the processing parameters of LMD process is very important as these influence the evolving properties such as porosity and microstructure of the part produced. Porosity behaviour in LMD parts is seen as a defect in most engineering applications especially in structures, but it has been reported to be of great importance in healing process as well as proper integration of medical implants and body tissues in biomedical applications [5].

On the other hand, Titanium and its alloys exhibit a very special combination of properties and corrosion resistance that has made them desirable for critical and demanding industrial use, these include: aerospace, chemical, and energy industry. Titanium alloys are unique lightweight, high strength alloy that are structurally efficient for critical, high-performance application such as aircraft, jet engine parts, and airframe components [5]. Ti6Al4V is an important titanium alloy used as medical implants due to its superior corrosion resistance properties and good biocompatibility. Despite these properties, the modulus of elasticity of titanium is however higher than that of human bone. This high modulus of elasticity of titanium leads to mismatch in titanium implant and the host bone. Thus, the modulus of elasticity of titanium can however be reduced and then made to be as close as possible to human bone through the introduction of porosity in the bulk material.

Processing parameters in LMD process have proven to affect the porosity of deposited parts [6]-[8]. Health issues concerning alloying elements commonly used in the production of α -phase titanium alloys have also been raised; nickel and chromium are known to be metal allergens whereas the use of vanadium and aluminium has been linked to cytotoxic tissue reactions and potential neurological disorders, respectively [9], [10]. In addition, researchers in this area deal with randomly distributed pores in titanium alloys. The control of porosity, pore size, and distribution is necessary to obtain implants with mechanical properties close to those of bone and to ensure their

osseointegration [11], [12]. Furthermore, the convective effect, known as Marangoni flow, is an important factor that not only influences the melt pool geometry, but can as well contribute to defects such as lack of fusion, and porosity [13].

On the other hand, Boron carbide belongs to the important group of nonmetallic hard materials, which includes alumina, silicon carbide, and diamond. Although it was first synthesized over a century ago, in 1883 by Joly. The formula B_4C was assigned only in 1934. Boron carbide is an extremely hard material, inferior in hardness only to diamond and cubic boron nitride. In addition, it has a high melting point, high mechanical strength combined with low density, high neutron cross section, and it is a semiconductor [14]. Its high wear, impact resistance, and low specific weight make it suitable for application in ball mills, nozzle, wheel dressing tools, wire drawing dies, rocket propellant, and light weight armour plates. It can also be used as a reinforcing material for ceramic matrix composites. This material is also regarded as an excellent neutron absorption material in nuclear industry due to its high neutron absorption coefficient [15].

Furthermore, its hot hardness is better than that of diamond and cubic boron nitride. Because of high hardness, it is extensively used as a lapping agent in place of diamond. It was reported [15] that the development of hard metal cutting tools and high speed steels could not have been possible without the availability of boron carbide as a grinding medium.

Boron carbide is however a brittle and not especially impact resistant. Apart from machining operations, sintered B_4C find wide applications as sand blasting nozzles and hard ceramic bearings. In aerospace industry, boron carbide due to its capability to generate tremendous amount of heat in combination with oxygen is finding use as a rocket propellant. In nuclear industry, it is well accepted as a control and shielding material for neutrons due to its favourable absorption characteristics [16]. In this research study, the influence of laser power on the average pore size and the percentage porosity of titanium composites was investigated. It was however observed that, increasing the laser power of the composites resulted in a decrease in the percentage porosity provided that all other process parameters were kept constant throughout the experiment.

II. EXPERIMENTAL PROCEDURE

The experimental materials involved in this study were Ti6Al4V powder and B_4C powder supplied by Alfa Aesar Company in Germany. The LMD process was achieved with 3.0 KW Ytterbium fibre laser system with coaxial powder nozzles. A Kuka robot was used to carry both the laser and powder nozzles and as well controls the deposition process. The rectangular Ti6Al4V substrate with dimensions 102 mm x 102 mm x 7 mm is prepared for the laser metal deposition of the mixture powders. Ti6Al4V alloy samples were sandblasted and cleaned under tap water and then dried with acetone prior to the coating operation. Boron carbide, B_4C powder with particle size of between 22-59

μm , and the titanium alloy powder with particle size of 45-90 μm , were deposited in the ratio of 1:4 in weight percent.

The laser power employed was varied between 800 W and 2400 W with 200 W interval. The beam spot size of 4 mm was employed to melt the surface of the samples in which 12 mm focal distance was maintained from the nozzle to the surface of the substrate. During the laser surface melting process, the powders were dissolved into the melted pool, leading to alloying the surface of the samples with boron carbide. To protect the melt pool from oxidation during laser deposition process, argon gas was initiated at a pressure of 2 MPa to provide shielding. The powders were fed through a nozzle which was coaxial with the laser beam.

Furthermore, the properties of Titanium alloy, Ti6Al4V used as substrate and as well as powder are described as follow: The substrate contains titanium alloy of Ti6Al4V while the powder contains properties with particle size range between 45 and 90 μm , spherical particle, and 99.6 % purity. On the other hand, the properties of boron carbide powder as-received are given as follow: density > 2.48 g/cm^3 , porosity < 0.5 %, average particle size < 15 μm , Vickers hardness 31 GPa, knoop hardness 29 GPa, and purity of > 99%. Figure 1 illustrates the photograph of the experimental setup for the laser metal deposition process.

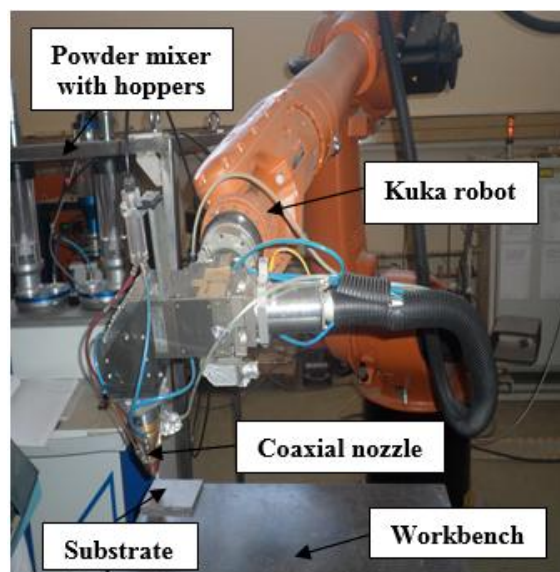


Fig. 1: Experimental setup

The gas assisted powder was delivered into the melt pool created by the laser on the substrate in order to generate a deposited track. Moreso, Figure 2 illustrates the laser metal deposition (LMD) process used for this research study.

The result of the preliminary experiment illustrate that at laser power of 2200 W, scanning speed of 1 m/min, powder flow rate of 6.68 g/min, and a gas flow rate of 2 l/min produced a fully dense, pore free with good metallurgical bonded deposit. These parameters were used as a benchmark in this study. The scanning speed, powder flow rate, and the gas flow rate were fixed and only the laser power was varied between 800 W and 2400 W. The processing parameters used in this research study were given in Table I.

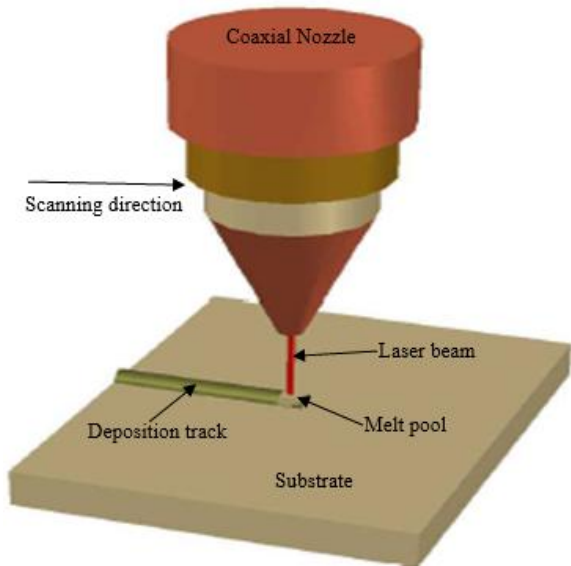


Fig. 2: Schematic view of laser metal deposition (LMD) process

TABLE I: EXPERIMENTAL MATRIX FOR THE LASER METAL DEPOSITION

Sample	Laser Power (W)	Scanning Speed (m/min)	Powder Flow Rate (g/min)	Gas Flow Rate (l/min)
X1	800	1	6.68	2
X2	1000	1	6.68	2
X3	1200	1	6.68	2
X4	1400	1	6.68	2
X5	1600	1	6.68	2
X6	1800	1	6.68	2
X7	2000	1	6.68	2
X8	2200	1	6.68	2
X9	2400	1	6.68	2

After the deposition process, the samples were laterally sectioned and mounted in resin. Hence the samples were ground, polished and etched according to the standard metallographic preparation of Titanium. The cut samples were studied under the Optical Microscope. Therefore, microstructural evaluation to study the porosity effect and the behaviours were conducted on the deposited tracks to determine the percentage porosity, pore count, and the maximum pore size of the composites. However, the processing parameters observed during the laser metal deposition (LMD) process are of utmost importance as they facilitated the properties such as porosity.

III. RESULTS AND DISCUSSION

The powder morphology for both titanium alloy (Ti6Al4V) and boron carbide (B₄C) materials used in this research work were shown in Figures 3 (a) and (b). While, the microstructure of the substrate used for the LMD process, as shown in Figure 4. The microstructure of the substrate was characterized by alpha and beta grain structure with the lighter part showing the alpha grains and the darker

part showing the beta grains. The alpha phase dominates more grain structures than the beta phase.

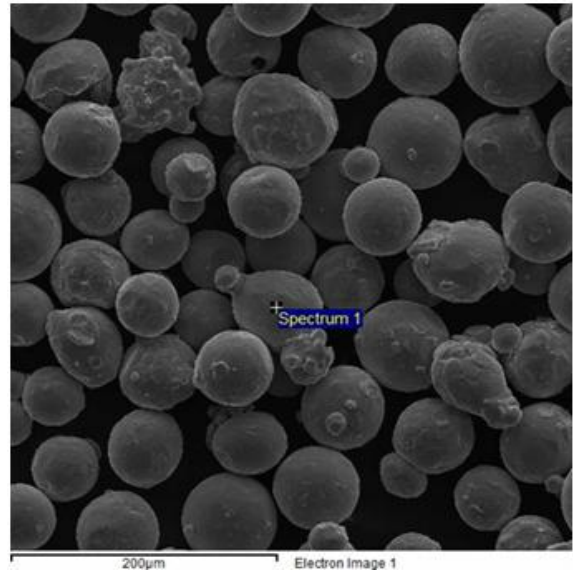


Fig. 3(a): Morphology of Ti6Al4V alloy powder

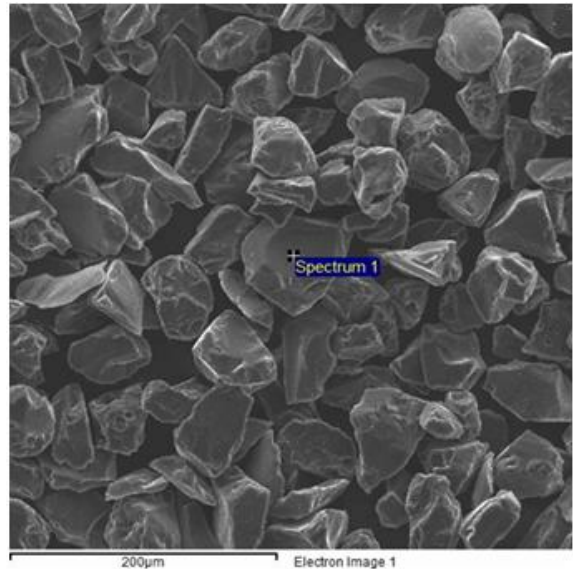


Fig. 3(b): Morphology of B₄C powder

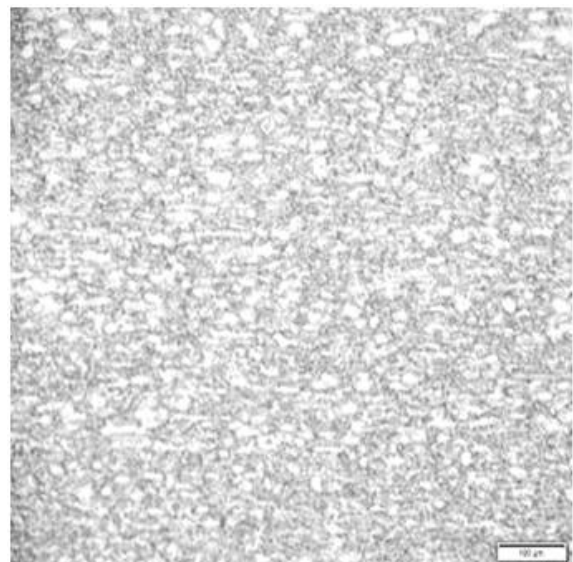


Fig. 4: Microstructure of the substrate

Figure 5 illustrates the physical appearance of the laser deposited Ti6Al4V-B₄C composites. From the single track deposition, it was observed that the width of deposit increased as the laser power increased due to the laser-material interaction.

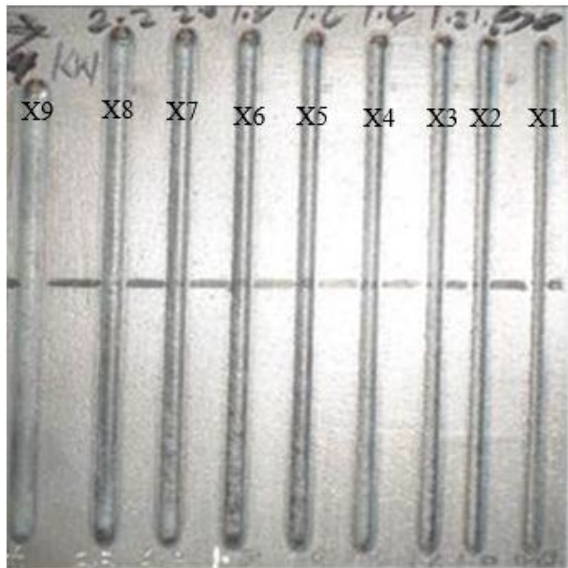


Fig. 5: The photograph of single track laser metal deposited Ti6Al4V-B₄C composites

Therefore, there were two kinds of pores observed after the deposition process, one was open pores that existed in the contact area between layers, and the other was the closed pores that existed inside the melted particles. Thus, these pores were associated with decrease in laser power during deposition process. Also, these pores experienced entrapment of gas such as oxygen which may have reacted with carbon to form carbon-oxide gas during the LMD process. Porosity effect and behaviour in the composites was obtained due to two factors, namely: (i) the unmelted powder particles in the composites after solidification, and (ii) the gas entrapment in the melt pool that was resulted in a hollow shape of porosity.

Microstructure of the samples at different laser power, as shown in Figures 6 (a) and (b). The degree of their porosities varies as the laser power increases and thereby arrived at a laser power in which no porosity was observed and then further experienced a significant amount of porosity as the laser power further increases.

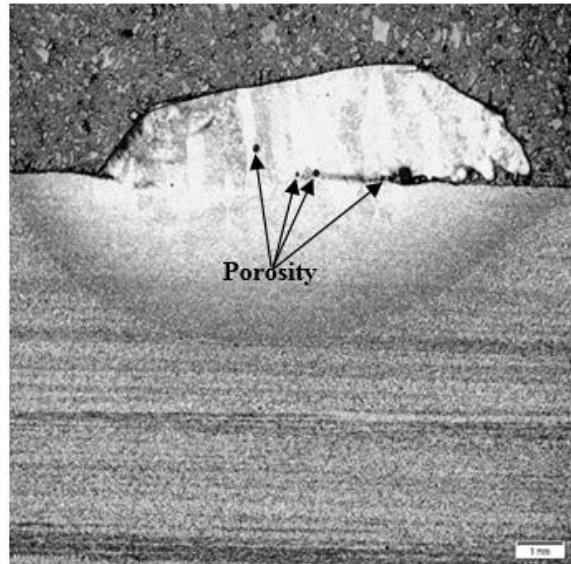


Fig. 6(a): Micrograph of sample X4 at laser power of 1400 W

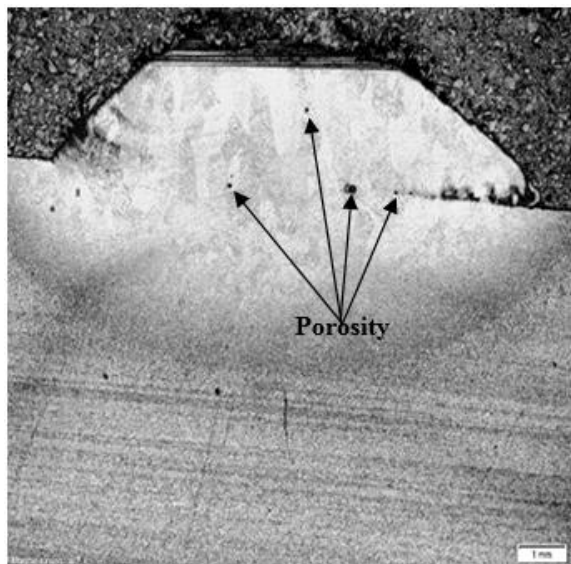


Fig. 6(b): Micrograph of sample X6 at laser power of 1800 W

The porosity at lower laser power of 1400 W can be attributed to insufficient melting of the powder particles. On the other hand, porosity at higher laser power was as a result of gas entrapment which however make the pore sizes become bigger. Figures 7 (a) and (b) illustrate the micrographs of sample X4 and X6 observed during the porosity analysis.

Interestingly, at laser power of 2200 W, there was no porosity observed in the characterized sample. Thus, there were no unmelted powder particles observed in the clad after solidification. Figure 8 however depicts that, the sample deposited at a laser power of 2200 W was characterized without porosity.

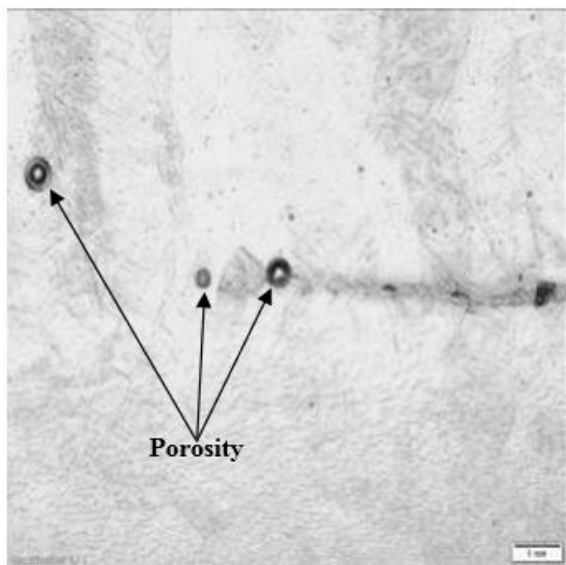


Fig. 7(a): Micrograph of sample X4 with high magnification at laser power 1400 W

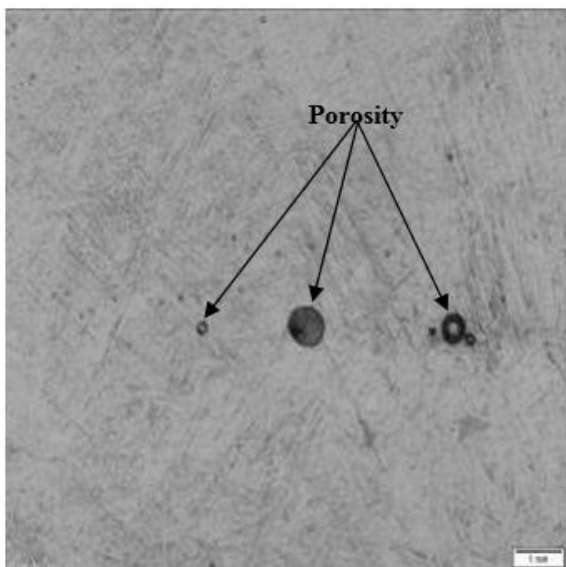


Fig. 7(b): Micrograph of sample X6 with high magnification at laser power 1800 W



Fig. 8: Micrograph of Ti6Al4V-B₄C composite of sample X8 at laser power of 2200 W

Moreso, the microstructure of this composite illustrates in Figure 8, was observed and characterized to be susceptible to porosity and thereby resulted in a fully densified deposit. Perhaps, there was a sufficient heat input generated by the laser system which however, provides adequate laser power to the melt pool whereby no unmelted powder remains in the molten pool after solidification. Table II presented the average percentage porosity and the maximum pore size of the samples.

TABLE II: AVERAGE PERCENTAGE POROSITY AND MAXIMUM PORE SIZE OF VARIOUS SAMPLES

Sample	Average porosity (%)	Maximum pore size (µm)
X1	0.45	158.01
X2	0.16	66.63
X3	0.12	33.96
X4	0.44	132.79
X5	0.31	153.47
X6	0.30	143.79
X7	0.09	64.45
X8	No porosity	Nil
X9	0.03	27.50

However, Figures 9 (a) and (b) presented the variation of average porosity as well as the maximum pore size for various samples at different laser power.

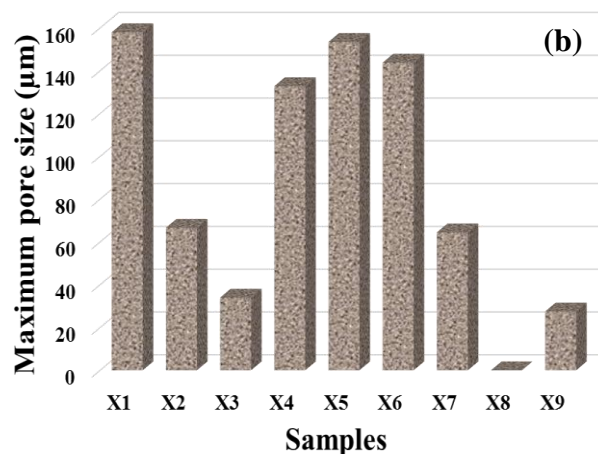
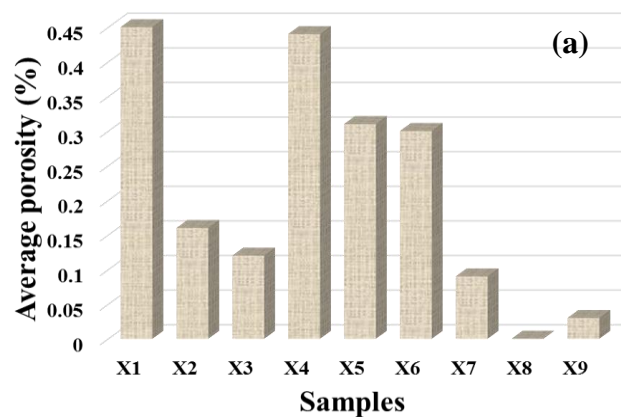


Fig. 9: The variation of (a) average porosity; and (b) maximum pore size for different samples

Figure 9 (a) represents that, as the laser power increases, the average porosity decreases from 0.45% to 0.09%. The reason for this behaviour was attributed due to the fact that at lower laser power between 800 W to 1800 W, there was insufficient heat input for melting the deposited powder onto the surface of the substrate. On the other hand, Figure 9 (b) represents that, the maximum pore size was observed to be associated with decreased-increased manner as the laser power increases. However, the porosity at higher laser power was observed due to gas entrapment in the melt pool prior solidification.

Within the range of process parameters used in this work, the level of porosity varied greatly in the deposited samples. Thus, the optimized process parameters to achieve minimum porosity were presented in Table III.

TABLE III: OPTIMIZED PROCESS PARAMETERS

Laser Power	Scanning Speed	Powder Flow Rate	Gas Flow Rate
2200 W	1 m/min	6.68 g/min	2 l/min
2400 W	1 m/min	6.68 g/min	2 l/min

IV. CONCLUSION

The porosity from lack of fusion is expected to be highly influenced by the laser power whereby increasing laser power would provide more energy to melt the powder, leading to reduced porosity. Thus, while porosity is considered as a defect in engineering applications, it is however regarded as an advantage in biomedical applications such as medical implants. The influence of laser power on the behaviour and degree of porosity was investigated in this study. At higher laser power, degree of porosity was reduced in terms of percentage average porosity whereby percentage porosity was drastically reduced from 0.45% to 0.03% which is a good achievement. On the other hand, the maximum pore sizes were observed to increase rapidly between sample X4, X5, and X6 as the laser power was increased which was attributed to gas entrapment in the melt pool before solidification. However, a low level of porosity degree in the deposit was achieved with the optimized process parameters. It is expected that porosity behaviour can be minimized by optimized setting of process parameters in laser metal deposition process. Therefore, a significant porous implant can be achieved by appropriate process parameters.

REFERENCES

[1] R. M. Mahamood, E. T. Akinlabi, M. Shukla and S. Pityana. Characterizing the Effect of Processing Parameters on the Porosity of Laser Deposited Titanium Alloy Powder. In: Proceedings of the International Multi-Conference of Engineers and Computer Scientists, vol. II, IMECS 2014, March 12-14, Hong Kong, 2014.

[2] E. F. Guasch, J. Wolff, M. Dent, M. N. Helder, E. A. J. M. Schulten, T. Forouzanfar, and J. K. Nulend. Application of Additive Manufacturing in Oral and Maxillofacial Surgery: American Association of Oral and Maxillofacial Surgeons, Journal of Oral Maxillofacial Surgery, 2015.

[3] R. M. Mahamood and E. T. Akinlabi. Processing Parameters Optimization for Material Deposition Efficiency in Laser Metal Deposited Titanium Alloy. Lasers Manufacturing Material Process, vol. 3, pp. 9–21, 2015.

[4] J. A. Slotwinski, E. J. Garboczi, P. E. Stutzman, C. F. Ferraris, S. S. Watson, and M. A. Peltz. Characterization of Metal Powders Used for Additive Manufacturing. Journal of Research of the National Institute of Standards and Technology: vol. 119, 2014.

[5] R. M. Mahamood, E. T. Akinlabi, M. Shukla and S. Pityana. Effect of Laser Power on Material Efficiency, Layer Height and Width of Laser Metal Deposited Ti6Al4V. In: Proceedings of the World Congress on Engineering and Computer Science 2012 vol. II, WCECS 2012, October 24-26, San Francisco, USA, 2012.

[6] L. M. Vasconcellos, F. N. Oliveira, D. O. Leite, L. G. Oliveira Vasconcellos, R. F. Prado, C. J. Ramos, M. L. Alencastro, C. A. Alves Cairo and Y. R. Carvalho. Novel Production Method of Porous Surface Ti Samples for Biomedical Application. Journal of Material Science: Mater Med, vol. 23, pp. 357–364, 2011.

[7] X. P. Fan, B. Feng, Y. L. Di, J. X. Wang, X. Lu and J. Weng. Graded Porous Titanium Scaffolds Fabricated Using Powder Metallurgy Technique. Powder Metallurgy and Metal Ceramics, vol. 51, No. 5–5 (485), pp. 153–159, 2012.

[8] L. M. R. Vasconcellos, D. O. Leite, F. O. Nascimento, L. G. O. Vasconcellos, M. L. A. Graça, Y. R. Carvalho, C. A. Alves Cairo. Porous Titanium for Biomedical Applications: An experimental study on rabbits. Med Oral Patol Oral Cir Bucal, vol. 15 (2), 2010.

[9] A. W. Nugroho, G. Leadbeater and I. J. Davies. Processing of a Porous Titanium Alloy from Elemental Powders Using a Solid State Isothermal Foaming Technique. Journal of Material Science: Mater Med, vol. 21, pp. 3103–3107, 2010.

[10] M.V. Oliveira, L.C. Pereira and C.A.A. Cairo. Porous Structure Characterization in Titanium Coating for Surgical Implants. Materials Research, vol. 5, No 3, pp. 269-273, 2002.

[11] A. Barbas, A. S. Bonnet, P. Lipinski, R. Pesci and Guillaume Dubois. Development and Mechanical Characterization of Porous Titanium Bone Substitutes. Journal of the Mechanical Behaviour of Biomedical Materials, vol. 9, pp. 34-44, 2012.

[12] L. Reig, C. Tojal, D. J. Busquets and V. Amigo. Microstructure and Mechanical Behaviour of Porous Ti–6Al–4V Processed by Spherical Powder Sintering. Journal of Materials, vol. 6, pp. 4868-4878, 2013.

[13] G. K. L. Ng, A. E. W. Jarfors, G. Bi and H. Y. Zheng. Porosity Formation and Gas Bubble Retention in Laser Metal Deposition. Applied Physics A: Material Science and Processing, vol. 97, pp. 641-649, 2009.

[14] N. Cho. PhD Thesis: Processing of Boron Carbide. School of Materials Science and Engineering Georgia Institute of Technology, August 2006.

[15] A. K. Khanra. Production of Boron Carbide Powder by Carbothermal Synthesis of Gel Material. Bull. Mater. Sci., vol. 30, No. 2, pp. 93–96, 2007.

[16] S. K. Singhal and B. P. Singh. Sintering of Boron Carbide under High Pressures and Temperatures. Indian Journal of Engineering & Materials Sciences, vol.13, pp. 129-134, 2006.